

Interior Layer Structure in the Newtonian Blown Film

J. J. Shepherd* J. C. Bennett†

28 September 2004

Abstract

In this paper, the techniques and methodology of singular perturbation theory are applied to an analysis of the film-blowing of an incompressible Newtonian film. An appropriate, physically relevant small parameter is identified in the problem, and the method of matched asymptotic expansions is used to obtain a straightforward closed-form approximate expression for the film profile throughout the blown region. This may then be used to calculate such related quantities as the film thickness variation, and the film speed. The results of applying this closed-form expression are compared with numerical calculations using the package Maple, and it is shown that the two methods show encouraging consistency.

Contents

1	Introduction	2
2	Governing Equations	4
3	Numerical Results	5
4	Perturbation Analysis	7
5	Results and Discussion	12

*School of Mathematical and Geospatial Sciences, Royal Melbourne Institute of Technology, Melbourne, AUSTRALIA. jshep@rmit.edu.au

†School of Mathematical and Geospatial Sciences, Royal Melbourne Institute of Technology, Melbourne, AUSTRALIA. s2111773@student.rmit.edu.au

1 Introduction

In this paper, we present a mathematical analysis of the simplest model of the *film-blowing* process, the widely-used industrial process employed to manufacture the thin polymer film widely used in commercial and domestic applications. In reality, any full analysis of the most realistic models of film-blowing would involve highly nonlinear problems, reflecting the complex physical and chemical changes occurring during the manufacturing process. However, the relatively unsophisticated model we analyse here avoids many of the mathematical difficulties associated with more realistic models, at the same time retaining a lot of the characteristic solution structure observed in these.

Prior to considering the mathematical details of this simple model, we describe the essential features of the industrial manufacturing process itself. These are displayed schematically in Figure 1. A thin annular die of radius R_0 , width E_0 extrudes a tube of molten polymer film at a constant velocity U_0 . Application of an internal pressure difference ΔP causes this thin film tube to expand to an increased radius, as shown. At the same time, this tube or *bubble* of polymer is cooled by external air jets from an air ring located above the die, causing the film to solidify, eventually reaching a constant radius R_{D_0} with thickness E_{D_0} at the *freezeline*, where its speed is U_{D_0} . Subsequently, the overall bubble shape remains unaltered; with the tube of thin film being rolled flat as a double layered film and drawn off on to an overhead roller.

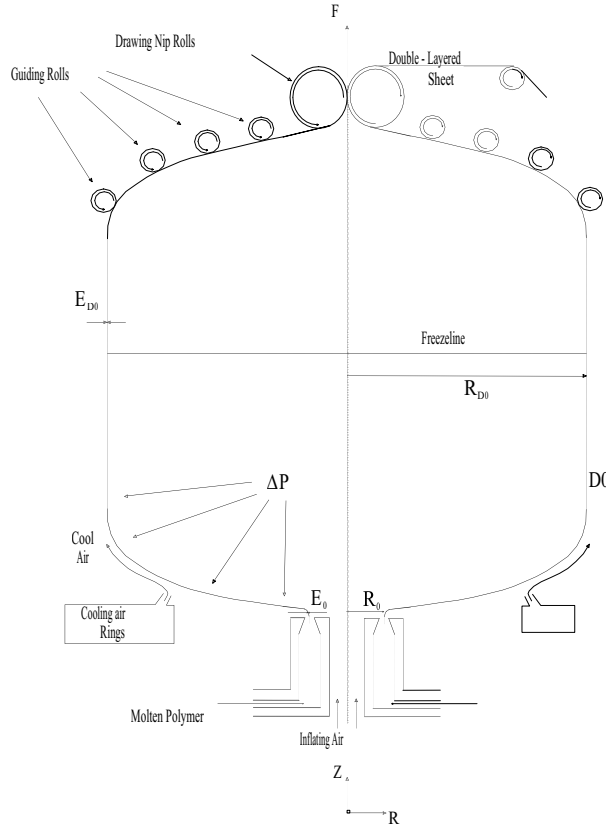


Figure 1: Schematic of film blowing process.

It occurs that for a physically realistic range of values of the significant parameters of the system, this film bubble radius expansion occurs over a relatively small part of the overall bubble region. Thus, we may view this localized expansion region as an *interior layer* region; and we might expect appropriate asymptotic methods based on a suitably chosen small parameter to yield approximations to the radius profile and other related quantities.

In what follows, we will make the assumption that the material comprising the bubble is an incompressible Newtonian fluid, of constant viscosity η_0 . Further, we will ignore the effects of gravity on the film, so that it may be viewed as a thin shell under tension only from the drawing rolls and the imposed internal pressure ΔP . Moreover, we will assume that the bubble is in equilibrium, so that the blowing process is steady, while temperature variations are negligible; i.e., the process proceeds isothermally.

As we noted above, while these are severe simplifications of the real-world film blowing process, they lead to a mathematical model displaying the overall features of more sophisticated ones.

2 Governing Equations

The equations describing the film blowing process for materials displaying a range of complexity are well-represented in the literature [4]. For the present investigation, we will consider only the relatively simple situation described above - the steady, isothermal, gravity-free dilation of an incompressible Newtonian sheet. Under the assumption of axial symmetry, the only relevant spatial variables become the radial distance R , measured transverse to the bubble axis; and axial distance, Z , measured along that axis from the polymer extrusion die. Consequently, the state of the film may be described completely by the bubble radius $R(Z)$, its meridional speed $U(Z)$, the film thickness $E(Z)$ and the tension $F(Z)$; all depending only on the axial variable Z , with Z ranging from $Z = 0$ at the injection point (i.e., at the die) to $Z = D_0$ at the freezeline.

Introducing the dimensionless variables z , $r(z)$, $u(z)$, $e(z)$, and $f(z)$ defined by

$$z = \frac{Z}{D_0}, \quad r = \frac{R}{R_0}, \quad u(z) = \frac{U(Z)}{U_0}, \quad e(z) = \frac{2\pi R_0 U_0 E(Z)}{Q}, \quad f(z) = \frac{F(Z) R_0}{\eta_0 Q} \quad (1)$$

where Q is the volume flow rate of fluid in the film, η_0 is (as above) its viscosity, while R_0 , E_0 , U_0 and ΔP are as described above, allows us to express the momentum and mass conservation equations as the nonlinear differential equation for $r(z)$

$$2C^2 r^2 (f_0 + B(r^2 - 1)) r'' - 6Cr' + 4Br^3 (1 + C^2 (r')^2) - r (f_0 + B(r^2 - 1)) (1 + C^2 (r')^2) = 0, \quad (2)$$

where the dimensionless quantities B , C , f_0 are defined by

$$B = \frac{\pi \Delta P R_0^3}{\eta_0 Q}, \quad C = \frac{R_0}{D_0}, \quad f_0 = \frac{F_0 R_0}{\eta_0 Q}, \quad (3)$$

respectively and $F_0 = F(0)$, together with the differential equation for $u(z)$;

$$2C(2ru' + ur') - ru(f_0 + B(r^2 - 1))(1 + C^2(r')^2) = 0; \quad (4)$$

the algebraic equation for $e(z)$;

$$r(z)u(z)e(z) = 1; \quad (5)$$

and the force condition for $f(z)$:

$$f(z) = f_0 + B(r^2 - 1). \quad (6)$$

Appropriate boundary conditions at the ends of the bubble are

$$r(0) = 1, \quad r'(1) = 0, \quad (7)$$

$$u(0) = 1, \quad (8)$$

and

$$e(0) = 1, \quad (9)$$

We note that Equation (2), while highly nonlinear, is a single equation for $r(z)$ that may, in principle, be solved subject to the boundary conditions (7).

This solution may then be applied to (4) and (8), to obtain expressions for the film speed $u(z)$, while (5), (6) and (9) yield the film thickness $e(z)$ and tension $f(z)$.

3 Numerical Results

The nonlinear boundary value problem comprising the differential equation (2) together with the boundary conditions (7) cannot be solved analytically; and numerical methods must be employed. Typically, we expect a shooting method to be appropriate, using initial conditions

$$r(0) = 1, \quad r'(0) = k, \quad (10)$$

with k being adjusted to meet the second boundary condition at $z = 1$. This was the approach reported in [5], [6] and [7]. However, in the present case, we experienced instability due to the zero slope condition at $z = 0$ - as reported in [1] and [2]. Thus, a backward shooting technique was employed, by which (2) was integrated from $z = 1$ back to $z = 0$, with initial conditions

$$r(1) = \rho_{BU}, \quad \text{and} \quad r'(1) = 0, \quad (11)$$

where ρ_{BU} is the *blow up ratio*, defined by

$$\rho_{BU} = \frac{R_{D_0}}{R_0}. \quad (12)$$

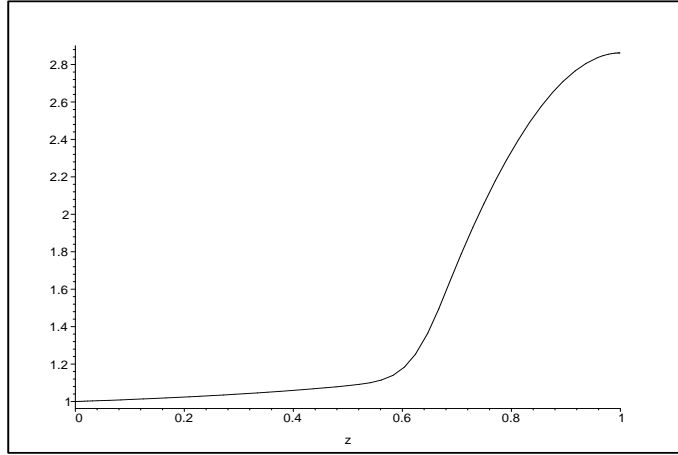


Figure 2: Typical bubble radius profile $r(z)$.

A typical bubble radius profile is shown in Figure 2 above. The Figure shows clearly the structure of the bubble radius profile. As can be seen, the radius changes relatively slowly for some distance from the die ($z = 0$). There then follows a restricted region of rapid expansion, followed by a third region of again relatively slow variation, until the freezeline ($z = 1$) is reached. In this investigation, we are interested in discovering how this region of rapid change ('interior layer') is derived from the differential equation (2), which of the physical parameters B , C , f_0 define its structure; and how we may obtain useful approximations to the radius profile for realistic parameter values. Figure 3 below displays the radius profile for fixed values of B and f_0 , and decreasing values of C - $C = 0.15, 0.135, 0.115, 0.095$ and 0.08 .

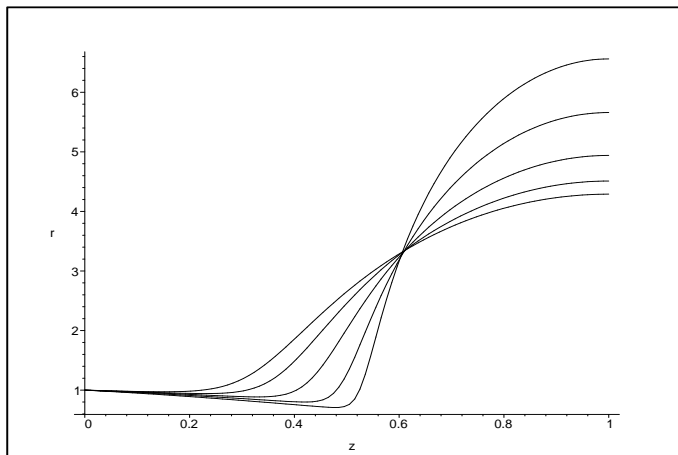


Figure 3: Radius profile $r(z)$ for decreasing C -values. Smaller C -values correspond to steeper slopes in the transition region .

It is apparent from this that the interior layer structure arises as a result of the limiting process $C \rightarrow 0$; although precisely how this comes about is not clear, as yet. However, it seems that a perturbation analysis based on this limit may yield useful results. Thus, in what follows, we employ appropriate perturbation techniques to construct a useful approximation to the film bubble profile $r(z)$.

4 Perturbation Analysis

We will find it convenient to rearrange the differential equation (2) in the form

$$C^2 r'' + \alpha(r, r', C) r' + \beta(r) = 0, \quad (13)$$

where

$$\alpha(r, r', C) = \frac{C^2 (3Br^2 - f_0 + B) r r' - 6C}{2r^2 (f_0 + B (r^2 - 1))}$$

and

$$\beta(r) = \frac{(3Br^2 - f_0 + B) r}{2r^2 (f_0 + B (r^2 - 1))}.$$

In what follows, we assume that the interior layer (region of rapid bubble radius variation) is centred at $z = a$, and that $r(a) = \lambda$, where a and λ are to be determined. For the numerical results of Section 3 above, we expect (roughly) $a \approx 0.6$, $\lambda \approx 1.2$. Then, the solution of (13) on $[0, 1]$ may be viewed as the union of solutions $r_1(z)$, $r_2(z)$ on $[0, a]$ and $[a, 1]$, with boundary conditions

$$r_1(0) = 1, r_1(a) = \lambda \quad \text{and} \quad r_2(a) = \lambda, r_2'(1) = 0 \quad (14)$$

respectively, together with suitable smoothness conditions at $z = a$. For $C \rightarrow 0$, the structure of these solutions depends heavily on the sign of $\alpha(r, r', C)$; which, in general, cannot be found until the (unknown) solution $r(z)$ is itself found. However, for the numerical results of Section 3, $\alpha(r, r', C)$ may be plotted over all of $[0, 1]$ and for a range of (small) C -values, as in Figure 4 below.

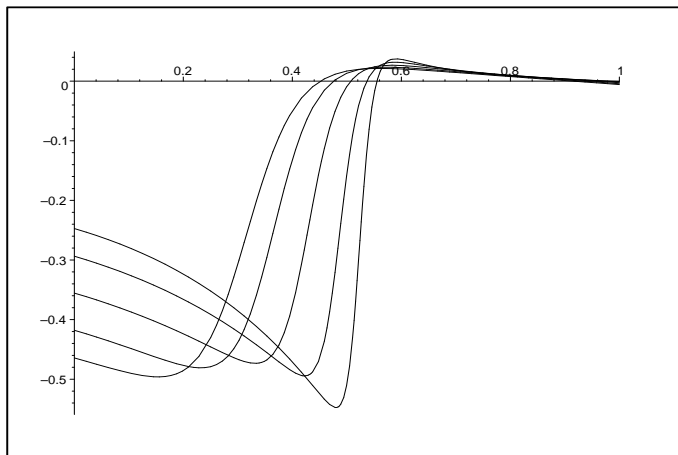


Figure 4: Variation of $\alpha(r, r', C)$ of Equation (13). Smaller C - values correspond to steeper slopes in the transition region ($z \approx 0.5$).

It is clear that, for small C , there exists a point $z^* \approx a$ at which α vanishes; and $a < 0$ on $[0, z^*)$, while $\alpha > 0$ (though it is small) on $(z^*, 1]$. Clearly, z^* varies with C , though not greatly; so if we choose $z^* \approx a$ as a leading approximation, we might expect it to be plausible that solutions r_1, r_2 of (13) on $[0, a]$ and $[a, 1]$ satisfying (14) are mimicked, in some sense, by those of the semilinear equation

$$C^2 r'' + k(z)r' + \beta(r) = 0, \quad (15)$$

where $k(z)$ is a suitably chosen function such that $k(z) < 0$ on $[0, a)$, $k(z) > 0$ on $(a, 1]$ and $k(a) = 0$. If we recall that C , and, consequently, C^2 are to be viewed as small, we see from standard perturbation theory results [3], that such solutions will display a layer of thickness $O(\sqrt{C^2})$; i.e., $O(C)$ on either side of $z = a$. In each case, the method of matched expansions may be used to construct an approximation to the solution over each subinterval. The smoothness conditions applied at $z = a$ then yield values for a and λ ; and ultimately an approximation to the bubble profile function over the whole of the interval $[0, 1]$.

On $[0, a)$, and bounded away from $z = a$ as $C \rightarrow 0$, we see from Figure 3 that $r_1 \approx 1$, while $r_1', r_1'' = O(1)$. Thus, on this subinterval, we replace Equation (2) by

$$C^2 r_1'' - \frac{3Cr_1'}{f_0} + \frac{B - f_0}{2f_0} + \frac{3Br_1^3}{2f_0} = 0, \quad (16)$$

which is to be solved using a perturbation expansion in C^2 , subject to the boundary condition at $z = 0$.

In the $O(C)$ neighbourhood to the left of $z = a$, it is no longer true that $r'_1, r''_1 = O(1)$. In particular, r'_1 is large (and positive), and we seek an estimate of this quantity in the layer. We note from (4) that, for small C , $\alpha = 0$ when

$$r \approx \sqrt{\frac{f_0 - B}{3B}}$$

so that, in crossing the layer, r_1 goes from $r_1 \approx 1$ to the above value. Thus, we propose that a suitable estimate of r'_1 in the layer left of $z = a$ is

$$r'_1 \approx \frac{\sqrt{\frac{f_0 - B}{3B}} - 1}{C}, \quad (17)$$

while we use the estimate $r_1 \approx 1$ there as well. Thus, on $[0, a)$, and bounded away from $z = a$, we estimate α as

$$\alpha = \frac{C}{2f_0} \left[(4B - f_0) \left(\sqrt{\frac{f_0 - B}{3B}} - 1 \right) - 6 \right] \quad (18)$$

and since $\alpha = 0$ at $z = a$, we estimate α' in the layer region to the left of $z = a$ as

$$\begin{aligned} \alpha' &= \frac{0 - \frac{C}{2f_0} \left[(4B - f_0) \left(\sqrt{\frac{f_0 - B}{3B}} - 1 \right) - 6 \right]}{C} \\ &= \frac{6 - (4B - f_0) \left(\sqrt{\frac{f_0 - B}{3B}} - 1 \right)}{2f_0} \\ &= M, \text{ say.} \end{aligned} \quad (19)$$

So, throughout the layer, an estimate of α is

$$\alpha \approx M(z - a) \quad (20)$$

so that in the layer to the left of $z = a$, the governing differential equation for r_1 is

$$C^2 r''_1 + M(z - a)r'_1 + \beta(r_1) = 0, \quad (21)$$

where M is as above. Thus, in terms of the local variable $\xi = (a - z)/C$, the differential equation governing an approximate solution in the layer left of $z = a$ is

$$\frac{d^2 \tilde{r}_1}{d\xi^2} + M\xi \frac{d\tilde{r}_1}{d\xi} = 0 \quad (22)$$

where $\tilde{r}_1(\xi, C) \equiv r_1(a - C\xi, C)$, and primes denote derivatives taken with respect to ξ . This is to be solved approximately using a perturbation expansion subject to the boundary condition $\tilde{r}_1(0, C) = \lambda$. If the results of this calculation and that for r_1 above are combined using the matching process, a leading-order approximation to r_1 valid over all of $[0, a]$ (i.e., the leading term of a *composite* expansion) is found to be

$$r_{1c}(z, C) = \phi(z, C) + (\phi(a, C) - \lambda) \operatorname{erf} \left(\frac{\sqrt{2M}(a-z)}{2C} \right) + \lambda - \phi(a, C) \quad (23)$$

where

$$\phi(z, C) = \left[\left(1 - \frac{3B}{f_0 - B} \right) e^{(\frac{f_0 - B}{3C})z} + \frac{3B}{f_0 - B} \right]^{-\frac{1}{2}} \quad (24)$$

and M is as given above.

On the interval $[a, 1]$, the situation is different. As the profiles of Figure 4 show, while $\alpha > 0$ there, it is also very small there. In fact, it seems to be vanishingly small as $C \rightarrow 0$ over much of the subinterval. Thus, while standard theory would indicate a layer to the right of, and adjacent to $z = a$, we anticipate this effect to be small; and, in fact negligible.

We thus seek a simple equation whose solution is readily obtained, and which (hopefully) approximates that of the full nonlinear equation (2) over all of $[a, 1]$. The profiles of Figure 3 imply that, on this subinterval, $r(z)$ does not vary a lot, while $r'(z)$ is bounded there. In fact, a reasonable estimate over $[a, 1]$ is given by $r(z) \approx r(1) = \rho_{BU}$, $\rho_{BU} = r(1)$ is the *blow-up ratio*, given above. These considerations lead us to propose that, on $[a, 1]$, the nonlinear equation (2) be replaced by the approximate equation

$$C^2 r_2'' - \frac{3C r_2'}{\rho_{BU}^2 (f_0 + B(\rho_{BU}^2 - 1))} - \frac{(f_0 - B(3\rho_{BU}^2 + 1))}{2\rho_{BU} (f_0 + B(\rho_{BU}^2 - 1))} = 0. \quad (25)$$

which is readily solved subject to the second of the boundary conditions in (14), to give a leading order approximation to the radius profile on $[a, 1]$ as

$$r_2(z, C) = \lambda + \frac{1}{18} \rho_{BU}^3 \sigma \gamma (e^{\eta(z, C)} - e^{\eta(a, C)}) - \frac{\rho_{BU}}{6C} \gamma (z - a), \quad (26)$$

where

$$\sigma = (f_0 + B(\rho_{BU}^2 - 1))$$

and

$$\gamma = (f_0 - B(3\rho_{BU}^2 + 1))$$

and

$$\eta(z, C) = e^{\frac{3(z-1)}{C\sigma\rho_{BU}^2}}.$$

The boundary conditions (14) ensure that r_{1c} and r_2 join continuously at $z = a$. A smooth join may be obtained (at least to leading order) by imposing the conditions

$$r'_{1c}(a) = r'_2(a); r_2(1) = \rho_{BU} \quad (27)$$

which serve to determine approximate values for a and λ , and ensure that the profile radius reaches the blow-up ratio at the freezeline.

An approximate film radius profile $r_c(z)$ valid over all of $[0, 1]$ may then be constructed as

$$r_c(z) = r_{1c}(z)(H(z) - H(z - a)) + r_2(z)(H(z - a) - H(z - 1)). \quad (28)$$

where $H(z)$ is the Heaviside function.

5 Results and Discussion

The approximations r_{1c} and r_2 were constructed as in the previous section, using the data set

$$B = 0.2, \quad C = 0.11, \quad f_0 = 0.736, \quad \rho_{BU} = 2.862. \quad (29)$$

The conditions (27) gave

$$a = 0.683712, \quad \lambda = 1.6165212, \quad (30)$$

and the overall approximation $r_c(z)$ was constructed as in (28).

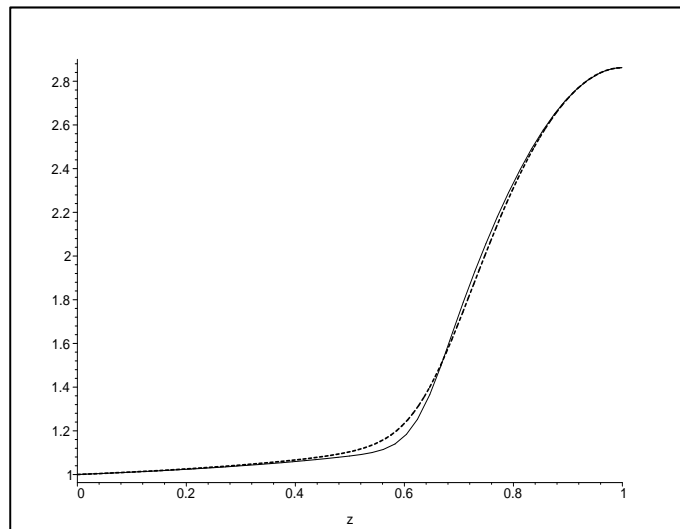


Figure 5: Comparison of bubble radius profiles as given by (28) and numerical calculations. The dotted curve is the numerical result.

The results of numerical calculations using the package *Maple* are compared with the results obtained above in Figure 5 above. Agreement between the two profiles seems quite good, given the somewhat rough estimates used in obtaining the approximating differential equations (16), (21) and (25). As anticipated, the discrepancy is greatest in the layer region. Nevertheless, both profiles have much the same structure, with the rapid transition centred about more or less the same point in each case. The analysis used here was motivated by a desire to obtain a straightforward analytical expression for the radial film bubble profile, that minimized calculation, and provided reasonable accuracy. We feel that the above calculations have achieved this, to a large degree.

References

- [1] J C Bennett, Interior Layer Structure in the Blown Newtonian Film, Honours Thesis, School of Mathematical and Geospatial Science, RMIT, 2004 (in preparation).
- [2] X.-L. Luo, R. I. Tanner, A Computer Study of Film Blowing, *Polymer Engineering and Science*, Vol 25, no 10, 1985, pp 620-629.
- [3] A. H. Nayfeh, *Perturbation Methods*, John Wiley and Sons, 1973.

- [4] J. R. A. Pearson, *Mechanics of Polymer Processing*, Elsevier Applied Science Publishers, 1985.
- [5] J J Shepherd, H J Connell and D C H Tam, An interior layer in a film-blowing problem, *Proceedings of the Fifth Biennial Engineering Mathematics and Applications Conference (EMAC2002)*, M Pember-ton, I Turner, P Jacobs (eds), The Institution of Engineers Australia, Brisbane, Queensland (2002), pp 181-186
- [6] D C H Tam, *Mathematical Analysis of the Blown Newtonian Film*, MAppSc Thesis, RMIT, 2003
- [7] D C H Tam, J Shepherd and H Connell, Modelling the film blowing process, *Proceedings of the Fourth Biennial Engineering Mathematics and Applications Conference (EMAC2000)*, R L May, G F Fitz-Gerald, I H Grundy (eds), The Institution of Engineers Australia, Melbourne (2000), pp 271-274.